Entropy-Driven Polar Ordering in Single-Phase Ferroelectrics

Jian Liu(刘剑),[1,2*] and Shi Liu(刘仕)[3,4†]

[1]*Institute of Frontier and Interdisciplinary Science, Shandong University, Qingdao, Shandong, 266237, China*

[2]*School of Energy and Power Engineering, Shandong University, Jinan, Shandong, 250061, China*

[3]*Key Laboratory for Quantum Materials of Zhejiang Province, School of Science, Westlake University, Hangzhou, Zhejiang 310024, China*

[4]*Institute of Natural Sciences, Westlake Institute for Advanced Study, Hangzhou, Zhejiang 310024, China*

Landau theory of phase transitions as one of the most influential phenomenological theory predicts a guaranteed reduction of order parameter with increasing temperatures, corroborating the intuition that a system becomes less ordered driven by entropy and numerous experimental evidence. Herein, combining the Landau theory with quasi-harmonic phonon theory, we demonstrate that the vibrational entropy can drive a more polar ordered state even in a single-phase material. Supported by first-principles calculations, our theory reveals the intrinsic origin of the thermally enhanced spontaneous electric polarization in ferroelectric hydrogen-bonded molecular crystal croconic acid: the seemingly counterintuitive entropy loss from polar ordering is overcompensated by the entropy gain from molecular rotational disordering, highlighting that the Landau order parameter is not necessarily a viable measure of Boltzmann's entropy in ferroelectrics.

Keywords: Landau theory, pyroelectricity, croconic acid, first-principles calculations

---

*Jian.Y.Liu@sdu.edu.cn, †liushi@westlake.edu.cn

1. Introduction

The general theory of phase transitions developed by Landau[1] and Devonshire[2-4] (abbreviated as Landau theory hereafter) is a shining intellectual accomplishment with far-reaching impacts across a broad range of disciplines. The essence of Landau theory is to characterize the ordering media with a mesoscopic parameter, called order parameter (η), which measures the extent of deformation of the low-temperature phase relative to the high-temperature phase[5, 6]. The Landau free energy is a low-order ~~Taylor~~ series expansion in terms of η, and the simplest form reads $F(\eta,T) = F_0(T) + \frac{1}{2}\tilde{a}(T-T_C)\eta^2 + \frac{1}{4}b_0\eta^4$, where T is the temperature, $F_0(T)$ is the free energy of the reference high-symmetry phase at T, $\tilde{a}$ and b_0 are T-independent positive constants, and T_C is the phase transition temperature. The equilibrium condition $\partial F/\partial\eta = 0$ leads to the T-dependent η (i.e. $\eta_T = \sqrt{\tilde{a}(T_C - T)/b_0}$), predicting a monotonically reduced ordering with increasing T and a second-order phase transition at T_C. This is perfectly consistent with Boltzmann's entropy that measures the degree of disorder $S = k_B \ln \Omega$, where Ω is the number of accessible states the higher the temperature, the larger the disorder, and the higher the entropy.

The idea of entropy-driven ordering[7] therefore may seem counterintuitive but actually has a long history, dating back to Onsager's study on colloidal particles in 1949[8]. The key to the reconciliation lies in that our intuitive idea of order and disorder (e.g., crystalline solids are more ordered than isotropic liquids) does not necessarily align with Boltzmann's entropic measure of disorder. Most entropy-driven ordering processes occur in composite materials. For example, with increasing T, mixtures of colloidal rods can transform to more ordered states such as "lamellar" and "columnar" phases[9]. Recently, a temperature-driven transition from an isospin-unpolarized Fermi liquid to a correlated state (analogous to solid) with strongly fluctuating magnetic moments has been demonstrated in magic-angle twisted bilayer graphene[10, 11], resembling the famous Pomeranchuk effect[12]. The fundamental question we would like to answer is whether the entropy can be a driving force for the non-local ordering in simpler systems such as single-phase materials.

We first give a simple proof using an extended Landau model that the vibrational entropy in principle allows for enhanced polar ordering in ferroelectrics. The phenomenological Landau theory can be interpreted from the perspective of the lattice dynamics of the displacive phase transition[13, 14] in which the soft mode[15] acts as the order parameter η. The frequency of a phonon (of mode λ at wavevector $\vec{q}$) at T is renormalized due to anharmonic interactions and can be expressed to the second order of η as $\omega^2_{\vec{q}\lambda}(\eta) = \omega^2_{\vec{q}\lambda}(\eta)|_{\eta=0} + \alpha_{\vec{q}\lambda}\eta^2$. After incorporating the contribution of the T-dependent vibrational free energy $F_{\mathrm{vib}}(\eta,T)$ into the zero-Kelvin double-well potential $V(\eta)$, we obtain $F(\eta,T) = F_0(T) +$

$\frac{1}{2}(a_0 + a_T)\eta^2 + \frac{1}{4}b_0\eta^4$, where $a_0 < 0$ and a_T is temperature dependent and captures the free energy from phonons at finite temperatures. Within the quasi-harmonic approximation (QHA), a_T depends on T almost linearly following $a_T \sim \tilde{a}T$ ($a_T \sim \sum_{\vec{q}\lambda} \alpha_{\vec{q}\lambda} \frac{k_B T}{2\omega^2_{\vec{q}\lambda}(\eta)|_{\eta=0}}$) at high-$T$ limit[13]. From $\partial F/\partial \eta = 0$, we obtain $\eta_T = \sqrt{-(a_0 + a_T)/b_0}$. Evidently, the sign of the T dependence of η_T, $\frac{\partial \eta_T}{\partial T} = -\frac{\tilde{a}}{2b_0\eta_T}$, negatively correlates with the sign of $\frac{\partial a_T}{\partial T} = \tilde{a}$ (or $\alpha_{\vec{q}\lambda}$). Moreover, because $\frac{\partial S(T)}{\partial T} = -\frac{\partial^2 \left(F(T)|_{\eta_T}\right)}{\partial T^2} = \frac{\tilde{a}^2}{2b_0} + \frac{\partial S_0(T)}{\partial T} > 0$ (the first term is positive definite and the second term is positive as the entropy of the reference phase should increase with T), the total entropy is guaranteed to increase with increasing T regardless of the sign of $\tilde{a}$, thus fully complying with Boltzmann's measure of entropy. Therefore, there is no fundamental physics preventing a vibrational-entropy-driven polar ordering with increasing T provided $\tilde{a} < 0$ (Fig. S1a). The general expectation of reduced η_T with increasing T arises from the overall positive sign of $\alpha_{\vec{q}\lambda}$, that is, the phonon frequency scales with η and becomes smaller as η varies from one in the low-symmetry low-T phase to zero in the high-symmetry high-T phase, a typical feature of a "soft mode". In comparison, a phonon with negative $\alpha_{\vec{q}\lambda}$ will become harder with reducing η, referred to as a "stiff mode" hereinafter. We shall demonstrate in below that hydrogen-bonded molecular ferroelectric croconic acid (CRCA)[16] offers an ideal case of entropy-driven polar ordering in which low-frequency stiff modes lead to $\frac{\partial \eta_T}{\partial T} > 0$.

For ferroelectrics, η is generally associated with the spontaneous polarization P_S, the T variation of which gives rise to pyroelectricity $\Pi = \mathrm{d}P_S/\mathrm{d}T$, a fundamental material property responsible for a wide range of applications such as thermal imaging[17, 18] and pyroelectric energy harvesting[19, 20]. As a defining signature of entropy-driven polar ordering in single-phase ferroelectrics, P_S rises upon heating, leading to an *intrinsically positive* Π, referred to as the inverse pyroelectric effect in literature, which can enable novel device applications[21, 22]. Yet such *anomalous* Π was rarely considered feasible because nearly all known single-phase ferroelectrics exhibit intrinsically negative Π (a reducing P_S with increasing T) over the 100-year study on ferroelectricity. The discovery of above-room-temperature ferroelectricity in single-component CRCA[16, 23] has led to renewed interests in hydrogen-bonded molecular ferroelectrics. Among these ferroelectrics[24-28], CRCA exhibits the largest P_S (21 μC/cm^2)[16] that persists at room temperature and can be reversed at a relatively low coercive field, and hence has received tremendous attention from theoretical and experimental aspects. Most notably, CRCA exhibits an inverse Π of 55 ± 20 μC/(m^2·K) at room temperature[16] (comparable to many conventional pyroelectrics in absolute magnitude), while the underlying mechanism remains elusive.

2. Methods

2.1 Landau theory of phase transitions

Without loss of generality, we perform series expansion of $V(\eta)$ and $F_{\mathrm{vib}}(\eta, T)$ to the sixth order of η, namely

$$F(\eta, T) = F_0(T) + \frac{1}{2}(a_0 + a_T)\eta^2 + \frac{1}{4}(b_0 + b_T)\eta^4 + \frac{1}{6}(c_0 + c_T)\eta^6. \quad (1)$$

The explicit T dependence of a_T, b_T, and c_T stems from the renormalization of phonons and lies at the heart of our methodology. This is a natural extension of the so-called linear Grüneisen method[29, 30], the efficacy of which has been proven[31, 32]. We note that including the T dependence of high-order Landau expansion coefficients is not rare[33]. Yet, unlike the conventional approach where a priori knowledge of T_C was required to introduce the T dependence of $F(\eta, T)$ via $\tilde{a}(T - T_C)$, our approach directly computes Landau expansion coefficients without *ad hoc* assumptions of T dependence, and thus enables full first-principles predictions of η_T as well as T_C. One can readily see that when considering renormalizing effects of higher-order terms, $\frac{\partial \eta_T}{\partial T}$ has a nontrivial dependence on $\frac{\partial a_T}{\partial T}$, $\frac{\partial b_T}{\partial T}$, and $\frac{\partial c_T}{\partial T}$, and hence simply having $\frac{\partial a_T}{\partial T} < 0$ is not necessarily sufficient to guarantee a vibrational-entropy-driven polar ordering. We will introduce a more rigorous indicator for the sign of $\frac{\partial \eta_T}{\partial T}$ in below.

2.2 General theory of pyroelectricity

The pyroelectric coefficient Π at constant stress is conventionally decomposed into two parts: the primary Π_1 at constant external strain ε and the secondary Π_2

$$\Pi = \left(\frac{dP_S}{dT}\right)_\sigma = \Pi_1 + \Pi_2 = \left(\frac{\partial P_S}{\partial T}\right)_\varepsilon + \sum_i \left(\frac{\partial P_S}{\partial \varepsilon_i}\right)_T \left(\frac{\partial \varepsilon_i}{\partial T}\right)_\sigma. \quad (2)$$

The primary part accounts for the "clamped-lattice" pyroelectricity, i.e. the internal structural parameters vary with temperature while ions carry rigid Born effective charges (BECs). This is usually referred to as the rigid-ion model[34], as the electron-phonon renormalization of these effective charges is neglected. The secondary part accounts for the interplay between piezoelectricity e ($\partial P_S/\partial \varepsilon_i$) and thermal expansion α ($\partial \varepsilon_i/\partial T$).

2.3 Computational details

Density-functional theory total-energy calculations have been performed using the QUANTUM ESPRESSO package[35]. Phonons are calculated using density-functional perturbation theory[36]. Spontaneous polarization is calculated using the modern theory of polarization (Berry-phase method)[37-41]. For the electronic-structure calculations, we use the Perdew-Burke-Ernzerhof (PBE)[42] and the PBE revised for solids (PBEsol)[43] functionals for CRCA and $PbTiO_3$ respectively. To properly account for the van der Waals (vdW) interaction, the Grimme-D3 dispersion correction[44] is used. Ultrasoft pseudopotentials are taken from the PSLibrary[45]. The electronic wave-functions are expanded in a plane-wave basis with a kinetic energy cutoff of 120 Ry. For Brillouin-zone sampling, a 2×4×2 (6×6×6) *k*-point mesh is used for CRCA ($PbTiO_3$). All the structure figures are produced using VESTA[46]. The optimized lattice parameters are 8.83, 5.20, and 10.86 Å for CRCA, and 3.87 and 4.23 Å for $PbTiO_3$, respectively.

Ab initio molecular dynamics (AIMD) simulations are performed using a basis of linear combinations of localized atomic orbitals, as implemented in the SIESTA package[47]. CRCA is modelled by a supercell of 576 atoms (2×3×2 unit cells). A double-ζ polarized basis set is used with a mesh cutoff of 300 Ry for the real-space grid. For each AIMD simulation, a trajectory of 1 ps is used for production after an equilibration stage of 1 ps, with a time step of 0.5 fs. Simulations are performed within the canonical (*NVT*) and isothermal-isobaric (*NPT*) ensembles, with temperature and pressure controlled by the Nosé thermostat[48] and Parrinello-Rahman barostat[49], respectively. In the *NVT* simulation, lattice is clamped at its ferroelectric ground state value (and hence only Π_1 is included). In the *NPT* simulation, lattice thermal expansion is allowed (and hence Π_1 and Π_2 are both included). Temperature is gradually raised to facilitate achieving thermal equilibrium, i.e., the final snapshot (position and velocity) of the simulation at a lower temperature is used as the initial starting point of the simulation at a higher temperature. Spontaneous polarization is evaluated for the ensemble-averaged structure at each temperature.

3. Results and discussion

We compute (clamped-lattice) $F(\eta, T)$ at selected temperatures for CRCA and ferroelectric $PbTiO_3$ based on the extended Landau model. The study of $PbTiO_3$ serves as a benchmark given the abundant experimental and theoretical works on this archetypical ferroelectric (see also Supplemental Material[50], which includes Refs. [51-62]). As shown in Fig. 1, with increasing T, the double-well free energy landscape for $PbTiO_3$ becomes increasingly shallower with the free energy minimum shifting toward η of lower values, indicating normal primary pyroelectricity Π_1 of negative value and thermally suppressed polar ordering. The conventional Landau theory[14] assumes that higher-order expansion coefficients b_0 and c_0 are T-independent, and the sign of b_0 dictates the nature of the phase transition. This turns out to be a rather crude approximation even for $PbTiO_3$, as manifested in the marked T dependence of both $a(T)$ and $b(T)$ that go through a sign change with increasing T. The phase transition exhibits mostly an order-disorder character, namely it evolves from second-order to first-order at around 725 K as $b(T)$ turns from positive to negative, and eventually occurs at around 850 K as $a(T)$ turns from negative to positive. Above T_C, η_T (and hence P_S) jumps to zero (Fig. 2a). The predicted T_C is in line with the measured value (around 765 K)[63, 64]. These results demonstrate the validity and accuracy of our fully *ab initio* methodology for predicting finite-temperature thermal properties of ferroelectrics (see Fig. S2a for the calculated *T*-dependent dielectric susceptibility, and Fig. S2b for the calculated thermal expansion obtained from the global minimum of $F(\eta, \varepsilon, T)$).

In sharp contrast, our theory predicts a *positive* Π_1 of 40.5 μC/(m^2·K) in CRCA that is otherwise absent in the conventional Landau theory. For CRCA, counterintuitively, the free energy well becomes increasingly deeper while the corresponding η_T monotonically enhances with increasing T, in consistent with the experimental observation that the inverse pyroelectric response persists until around 450 K. We first offer a heuristic explanation to the thermally enhanced polar ordering in CRCA with the renormalization effect truncated to the second order $\omega^2_{\vec{q}\lambda}(\eta) = \omega^2_{\vec{q}\lambda}(\eta)|_{\eta=0} + \alpha_{\vec{q}\lambda}\eta^2$. With increasing T, the low-frequency phonons are predominantly excited according to the Bose-Einstein distribution. The entropic driving force requires η_T to vary with T such that these populated phonons will have reduced frequencies, thus maximizing

the vibrational entropy and minimizing the free energy. Simply put, the order of the system represented by η_T is driven thermally to a direction along which the phonon softening occurs. The thermally-driven polar ordering therefore could occur when low-frequency phonons are mostly stiff modes (phonon frequency negatively scales with η). We calculated $\omega_{\vec{q}\lambda}^2$ vs. η^2 for low-frequency modes of CRCA and $PbTiO_3$, respectively, as shown in Fig. 2b (see Fig. S3 for the corresponding normal modes). As expected, the low-frequency modes are soft modes in $PbTiO_3$ whereas being stiff modes in CRCA. We conclude that the polar ordering can indeed be driven by the vibrational entropy. The critical point here is that the order measured by the order parameter in the Landau model (often the one relevant for device applications) does not need to conform with the order associated with the total entropy in a thermodynamic system. Though for complex perovskites such as $CaTiO_3$ and $BiFeO_3$ two sets of order parameters have been included in the Landau model to better describe the free energy[65, 66], the demonstrated experiment-theory agreement of the pyroelectric response in CRCA indicates that a single order parameter is sufficient to well represent the free energy provided the expansion coefficients have the correct temperature dependence.

We find that the sign of $\frac{\partial \eta_T}{\partial T}$ directly correlates with the sign of $\frac{\partial F_{\text{vib}}(\eta,T)}{\partial \eta}$: with an increasing T, the minimization of $F(\eta, T)$ demands η_T evolving to a new state that has reduced $F_{\text{vib}}(\eta, T)$ and hence a negative $\frac{\partial F_{\text{vib}}(\eta,T)}{\partial \eta}$ naturally leads to a positive $\frac{\partial \eta_T}{\partial T}$. To gauge the response of F_{vib} ($\propto \ln \omega_{\vec{q}\lambda}$, see Methods) due to a perturbative change in η, we introduce the generalized Grüneisen parameter[29, 30] $\gamma_{\vec{q}\lambda}$ defined as $\gamma_{\vec{q}\lambda} = \frac{\partial \ln \omega_{\vec{q}\lambda}(\eta)}{\partial \eta}$, analogous to the Grüneisen parameter that describes the volumetric effect on the vibrational properties of a crystal. We note that $\gamma_{\vec{q}\lambda}$ captures higher-order effects of phonon renormalization going beyond $\alpha_{\vec{q}\lambda}$, and negative $\gamma_{\vec{q}\lambda}$ leads to the pursued entropy-driven polar ordering. Figure 2c shows the $\gamma_{\vec{q}\lambda}$ spectrum in both $PbTiO_3$ and CRCA. For $PbTiO_3$, low-frequency (below 100 cm^{-1}) phonons are associated with translational Pb motions[67]. These phonons of positive γ lead to negative (normal) Π_1, as found in most pyroelectrics. For CRCA, the low-frequency (below 200 cm^{-1}) stiff phonons, exhibiting negative γ, are associated with collective translations or rotations of the C_5O_5 molecular units bridged by the H atoms via the intermolecular hydrogen bonds O···H−O. Upon heating, the asymmetry of O···H−O enhances, namely as η_T increases the hydrogen bond O···H weakens (and becomes longer) while the covalent bond O−H strengthens. The weakened O···H thus reduces the frequencies of translations/rotations of C_5O_5 molecular units ($\gamma < 0$, gaining entropy), while the strengthened O−H is characterized by a blue shift of the stretching frequency (losing entropy). The entropy loss from the latter is more than compensated by the entropy gain from the former, complying with Boltzmann's measure of entropy that the overall entropy increases with increasing T. This provides a ferroelectric analog of the Onsager model for the nematic liquid crystal[8] where rod-shaped particles align orientationally to enable more translational entropy[68]. The unraveled mechanism is also corroborated with the bond valence method[69, 70] (Fig. S1b).

Our revised Landau model within QHA may reach its limit when the temperature is approaching T_C where the lattice vibrations could be highly anharmonic. To reveal the nature of the phase transition, we perform AIMD-*NVT* simulations. As shown in Fig. 3a, with the lattice clamped, P_S rises with T up to 300 K, further corroborating the entropy-driven polar ordering. To describe the hydrogen-bond-mediated P_S, we define an order parameter δ as the difference in the distance between the H atom and its two nearby terminal O atoms [namely d(O···H)−d(O−H), see the inset of Fig. 1a]. A larger δ (in magnitude) indicates a shorter O−H or a longer O···H. The T evolution of P_S is overall well correlated with that of the ensemble-averaged order parameter $\langle\delta\rangle$. Below 300 K, the probability distribution of δ exhibits a single peak, while $\langle\delta\rangle$ increases monotonically with increasing T, giving rise to an anomalously *positive* Π_1 of 30 μC/(m^2·K), agreeing well with the prediction from extended Landau model. Interestingly, $\langle\delta\rangle$ exhibits a crossover from *increase* to *decrease* at 300 K, due to the onset of proton transfer, and P_S gradually drops to zero at 700 K. We propose this crossover is due to the dominance of the configurational entropy at higher temperatures, the incorporation of which into our extended Landau model in principles allows an improved description. Notably, the probability distribution of δ at 700 K exhibits the superposition of two overlapping gaussian distributions, suggesting mostly an order-disorder character. The existence of two energetically metastable (but dynamically stable) antiferroelectric-like and ferrielectric-like structures (Fig. S4) is also indicative of such a transition.

Practical applications of ferroelectrics often require optimal design of phase transition properties. One example is the isotope effect in which substituting protons with heavier deuterons may enhance P_S as well as T_C[71], as a result of the so-called Ubbelohde effect[72]. Here we study the effect of phonon engineering[73, 74] enabled by hydrostatic pressure p in CRCA. The associated phenomenon, known as the barocaloric effect[75], is conventional ($\mathrm{d}T_C/\mathrm{d}p > 0$) and colossal in nonferroelectric plastic crystals[76, 77] with extensive molecular rotations whereas being inverse ($\mathrm{d}T_C/\mathrm{d}p < 0$) in many ferroelectrics[75] such as $PbTiO_3$ and $BaTiO_3$ exhibiting polar soft modes. A fundamental question arises regarding the nature of the barocaloric effect in CRCA, a molecular ferroelectric that has a polar soft mode and characteristics of a plastic crystal. In plastic crystals, pressure suppresses molecular rotations at a reduced volume and hence favors the orientationally ordered phase, resulting in a higher T_C. In CRCA, the suppression persists but the energy barrier of proton transfer that supports ferroelectricity is concurrently lowered such that T_C reduces with pressure (Figs. S5 and S6). We thus conclude that the large pressure tuning of T_C in CRCA ($T_C/\mathrm{d}p = -73$ K/GPa, one of the highest values in magnitude reported for barocaloric materials) resembles that in ferroelectrics such as perovskites[75] and ferrielectric ammonium sulphate[78].

Last but not least, due to the ubiquitous presence of hydrogen bonding, the seemingly rare entropy-driven polar ordering or similar phenomena may be found in other single-component hydrogen-bonded molecular ferroelectrics[79, 80]. We also offer two toy models based on the extended Landau theory showing that having negative $\frac{\partial a_T}{\partial T}$ can give rise to thermally-driven nonpolar-to-polar phase transition and emergent polar ordering respectively (Fig. S7). Different from other entropy-driven ordering phenomena such as the isospin Pomeranchuk effect in magic-angle graphene[10, 11] that requires two distinct degrees of freedom (isospin and phonon), here we show that one can take advantage of the vibrational frequency separation between polar and nonpolar phonon modes to realize vibrational-entropy-driven ordering. We expect the entropy-driven polar ordering will have broad implications from both fundamental and technological aspects. For example, for a ferroelectric with inverse pyroelectric effect, the application of an electric field along the polar direction will enhance the polar ordering but surprisingly *increases* the entropy, readily giving rise to an intrinsically *negative* electrocaloric effect[81]. A designed combination of both conventional and inverse pyroelectric or electrocaloric effects in devices may add to the performance[82, 83].

4. Conclusions

In summary, this work extends the conventional Landau theory by incorporating entropic contributions from lattice vibrations in a fully *ab initio* manner. The mechanism underlying the entropy-driven polar ordering (manifested as an inverse pyroelectric response) in CRCA is attributed to the hydrogen-bond-mediated interplay between the *disordering* of the low-frequency intermolecular translations/rotations and the *ordering* of the high-frequency intramolecular polar vibrations: entropy loss from the latter is more than compensated by entropy gain from the former. Even in single-phase materials (e.g., ferroelectrics), the order parameter does not necessarily correspond to the degree of ordering gauged by Boltzmann's entropy. This work may shed new light on novel pyroelectric/electrocaloric applications utilizing hydrogen-bonded molecular ferroelectrics, highlighting the potential of incorporating vibrational entropy for materials design.

Data availability

The main data supporting the findings of this study are available within the article and its supplementary information files.

References

[1] Landau L D and Lifshitz E M, *Statistical Physics*, Pergamon Press, Oxford, 1959.
[2] Devonshire A F 1949 *Philos. Mag.* **40** 1040
[3] Devonshire A F 1951 *Philos. Mag.* **42** 1065
[4] Devonshire A F 1954 *Adv. Phys.* **3** 85
[5] Zhang Y and Zhong F 2025 *Chin. Phys. Lett.* **42** 090001
[6] Yang Y-T and Luo H-G 2024 *Chin. Phys. Lett.* **41** 120501
[7] Adams M, Dogic Z, Keller S L and Fraden S 1998 *Nature* **393** 349
[8] Onsager L 1949 *Ann. N. Y. Acad. Sci.* **51** 627
[9] Mundoor H, Wu J-S, Wensink H H and Smalyukh I I 2021 *Nature* **590** 268
[10] Saito Y, Yang F, Ge J, Liu X, Taniguchi T, Watanabe K, Li J I A, Berg E and Young A F 2021 *Nature* **592** 220

[11] Rozen A, Park J M, Zondiner U, Cao Y, Rodan-Legrain D, Taniguchi T, Watanabe K, Oreg Y, Stern A, Berg E, Jarillo-Herrero P and Ilani S 2021 *Nature* **592** 214
[12] Pomeranchuk I 1950 *Zh. Eksp. Teor. Fiz* **20** 919
[13] Dove M T 1997 *Am. Mineral.* **82** 213
[14] Dove M T, *Introduction to Lattice Dynamics*, Cambridge University Press, Cambridge, 1993.
[15] Cowley R A 1980 *Adv. Phys.* **29** 1
[16] Horiuchi S, Tokunaga Y, Giovannetti G, Picozzi S, Itoh H, Shimano R, Kumai R and Tokura Y 2010 *Nature* **463** 789
[17] Whatmore R W 1986 *Rep. Prog. Phys.* **49** 1335
[18] Lang S B 2005 *Phys. Today* **58** 31
[19] Yang Y, Wang S, Zhang Y and Wang Z L 2012 *Nano Lett.* **12** 6408
[20] Yang Y, Guo W, Pradel K C, Zhu G, Zhou Y, Zhang Y, Hu Y, Lin L and Wang Z L 2012 *Nano Lett.* **12** 2833
[21] Geng W, Liu Y, Meng X, Bellaiche L, Scott J F, Dkhil B and Jiang A 2015 *Adv. Mater.* **27** 3165
[22] Park M H, Kim H J, Kim Y J, Moon T, Kim K D, Lee Y H, Hyun S D and Hwang C S 2016 *Adv. Mater.* **28** 7956
[23] Horiuchi S, Kobayashi K, Kumai R and Ishibashi S 2017 *Nat. Commun.* **8** 14426
[24] Koval S, Kohanoff J, Migoni R and Tosatti E 2002 *Phys. Rev. Lett.* **89** 187602
[25] Horiuchi S, Kumai R and Tokura Y 2011 *Adv. Mater.* **23** 2098
[26] Horiuchi S, Kagawa F, Hatahara K, Kobayashi K, Kumai R, Murakami Y and Tokura Y 2012 *Nat. Commun.* **3** 1308
[27] Katrusiak A and Szafrański M 1999 *Phys. Rev. Lett.* **82** 576
[28] Szafrański M, Katrusiak A and McIntyre G J 2002 *Phys. Rev. Lett.* **89** 215507
[29] Liu J and Pantelides S T 2018 *Phys. Rev. Lett.* **120** 207602
[30] Liu J, Fernández-Serra M V and Allen P B 2016 *Phys. Rev. B* **93** 081205
[31] Masuki R, Nomoto T, Arita R and Tadano T 2023 *Phys. Rev. B* **107** 134119
[32] Rostami S and Gonze X 2024 *Phys. Rev. B* **110** 014103
[33] Buessem W, Cross L and Goswami A 1966 *J. Am. Ceram. Soc.* **49** 33
[34] Peng Q and Cohen R E 2011 *Phys. Rev. B* **83** 220103
[35] Giannozzi P, Baroni S, Bonini N, et al. 2009 *J. Phys.: Condens. Matter* **21** 395502
[36] Baroni S, De Gironcoli S, Dal Corso A and Giannozzi P 2001 *Rev. Mod. Phys.* **73** 515
[37] King-Smith R and Vanderbilt D 1993 *Phys. Rev. B* **47** 1651
[38] Resta R, Posternak M and Baldereschi A 1993 *Phys. Rev. Lett.* **70** 1010
[39] Resta R 1994 *Rev. Mod. Phys.* **66** 899
[40] Bernardini F, Fiorentini V and Vanderbilt D 1997 *Phys. Rev. B* **56** R10024
[41] Resta R and Vanderbilt D 2007 *Physics of Ferroelectrics* 31
[42] Perdew J P, Burke K and Ernzerhof M 1996 *Phys. Rev. Lett.* **77** 3865
[43] Perdew J P, Ruzsinszky A, Csonka G I, Vydrov O A, Scuseria G E, Constantin L A, Zhou X and Burke K 2008 *Phys. Rev. Lett.* **100** 136406
[44] Grimme S, Antony J, Ehrlich S and Krieg H 2010 *J. Chem. Phys.* **132** 154104
[45] Dal Corso A 2014 *Comput. Mater. Sci.* **95** 337
[46] Momma K and Izumi F 2011 *J. Appl. Crystallogr.* **44** 1272
[47] Soler J M, Artacho E, Gale J D, García A, Junquera J, Ordejón P and Sánchez-Portal D 2002 *J. Phys.: Condens. Matter* **14** 2745
[48] Nosé S 1984 *J. Chem. Phys.* **81** 511
[49] Parrinello M and Rahman A 1981 *J. Appl. Phys.* **52** 7182
[50] See Supplemental Material at [URL] for detailed theory, discussion on secondary pyroelectric effect and inverse barocaloric effect in CRCA, and additional data validating the extended Landau model.
[51] Cohen R E 1992 *Nature* **358** 136
[52] Ishii F, Nagaosa N, Tokura Y and Terakura K 2006 *Phys. Rev. B* **73** 212105
[53] Stroppa A, Di Sante D, Horiuchi S, Tokura Y, Vanderbilt D and Picozzi S 2011 *Phys. Rev. B* **84** 014101
[54] Mukhopadhyay S, Gutmann M J, Jiménez-Ruiz M, Jochym D B, Wikfeldt K T, Refson K and Fernandez-Alonso F 2017 *Phys. Chem. Chem. Phys.* **19** 32216
[55] Mukhopadhyay S, Gutmann M and Fernandez-Alonso F 2014 *Phys. Chem. Chem. Phys.* **16** 26234
[56] Lang S B 1971 *Phys. Rev. B* **4** 3603
[57] Halliyal A, Bhalla A S, Markgraf S A, Cross L E and Newnham R E 1985 *Ferroelectrics* **62** 27
[58] Moya X, Kar-Narayan S and Mathur N D 2014 *Nat. Mater.* **13** 439
[59] Moya X and Mathur N D 2020 *Science* **370** 797
[60] Samara G A 1971 *Ferroelectrics* **2** 277
[61] Matsuki M, Yamada T, Yasuda N, Dekura S, Kitagawa H and Kimizuka N 2018 *J. Am. Chem. Soc.* **140** 291
[62] Božin E S, Malliakas C D, Souvatzis P, Proffen T, Spaldin N A, Kanatzidis M G and Billinge S J L 2010 *Science* **330** 1660

[63] Shirane G and Hoshino S 1951 *J. Phys. Soc. Japan* **6** 265
[64] Burns G and Scott B A 1973 *Phys. Rev. B* **7** 3088
[65] Gu Y, Rabe K, Bousquet E, Gopalan V and Chen L-Q 2012 *Phys. Rev. B* **85** 064117
[66] Xue F, Gu Y, Liang L, Wang Y and Chen L-Q 2014 *Phys. Rev. B* **90** 220101
[67] Ritz E T and Benedek N A 2018 *Phys. Rev. Lett.* **121** 255901
[68] Frenkel D 2015 *Nat. Mater.* **14** 9
[69] Brese N E and O'Keeffe M 1991 *Acta Cryst. B* **47** 192
[70] Brown I D 2009 *Chem. Rev.* **109** 6858
[71] Liu H-Y, Zhang H-Y, Chen X-G and Xiong R-G 2020 *J. Am. Chem. Soc.* **142** 15205
[72] Ubbelohde A and Gallagher K 1955 *Acta Cryst.* **8** 71
[73] Qian X, Zhou J and Chen G 2021 *Nat. Mater.* **20** 1188
[74] Guzmán-Verri G G, Brierley R T and Littlewood P B 2019 *Nature* **576** 429
[75] Mañosa L and Planes A 2017 *Adv. Mater.* **29** 1603607
[76] Li B, Kawakita Y, Ohira-Kawamura S, et al. 2019 *Nature* **567** 506
[77] Li F B, Li M, Xu X, Yang Z C, Xu H, Jia C K, Li K, He J, Li B and Wang H 2020 *Nat. Commun.* **11** 4190
[78] Lloveras P, Stern-Taulats E, Barrio M, Tamarit J L, Crossley S, Li W, Pomjakushin V, Planes A, Mañosa L, Mathur N D and Moya X 2015 *Nat. Commun.* **6** 8801
[79] Szafranski M 2011 *J. Phys. Chem. B* **115** 8755
[80] Pan Q, Liu Z B, Zhang H Y, Zhang W Y, Tang Y Y, You Y M, Li P F, Liao W Q, Shi P P and Ma R W 2017 *Adv. Mater.* **29** 1700831
[81] Xu H and Huang J 2025 *Chin. Phys. B* **34** 067702
[82] Hanrahan B, Espinal Y, Liu S, Zhang Z, Khaligh A, Smith A and Alpay S P 2018 *J. Mater. Chem. C* **6** 9828
[83] Yang C, Feng C, Lv P, Qian J, Han Y, Lin X, Huang S, Cheng X and Cheng Z 2021 *Nano Energy* **88** 106222

Acknowledgements

J.L. acknowledges the support from the National Natural Science Foundation of China (Grant No. 12174218 and 11904202). J.L. was supported by the Qilu Young Scholar Program of Shandong University. S.L. was supported by foundation of Westlake University and acknowledges the computational resource provided by Supercomputer Center at Westlake University.

Author contributions

J.L. and S.L. conceived the idea, analyzed the data, and wrote the manuscript. J.L. developed the theory and performed the calculations.

Competing interests

The authors declare no competing interests.

Additional information

Supplementary information. The online version contains supplementary material.

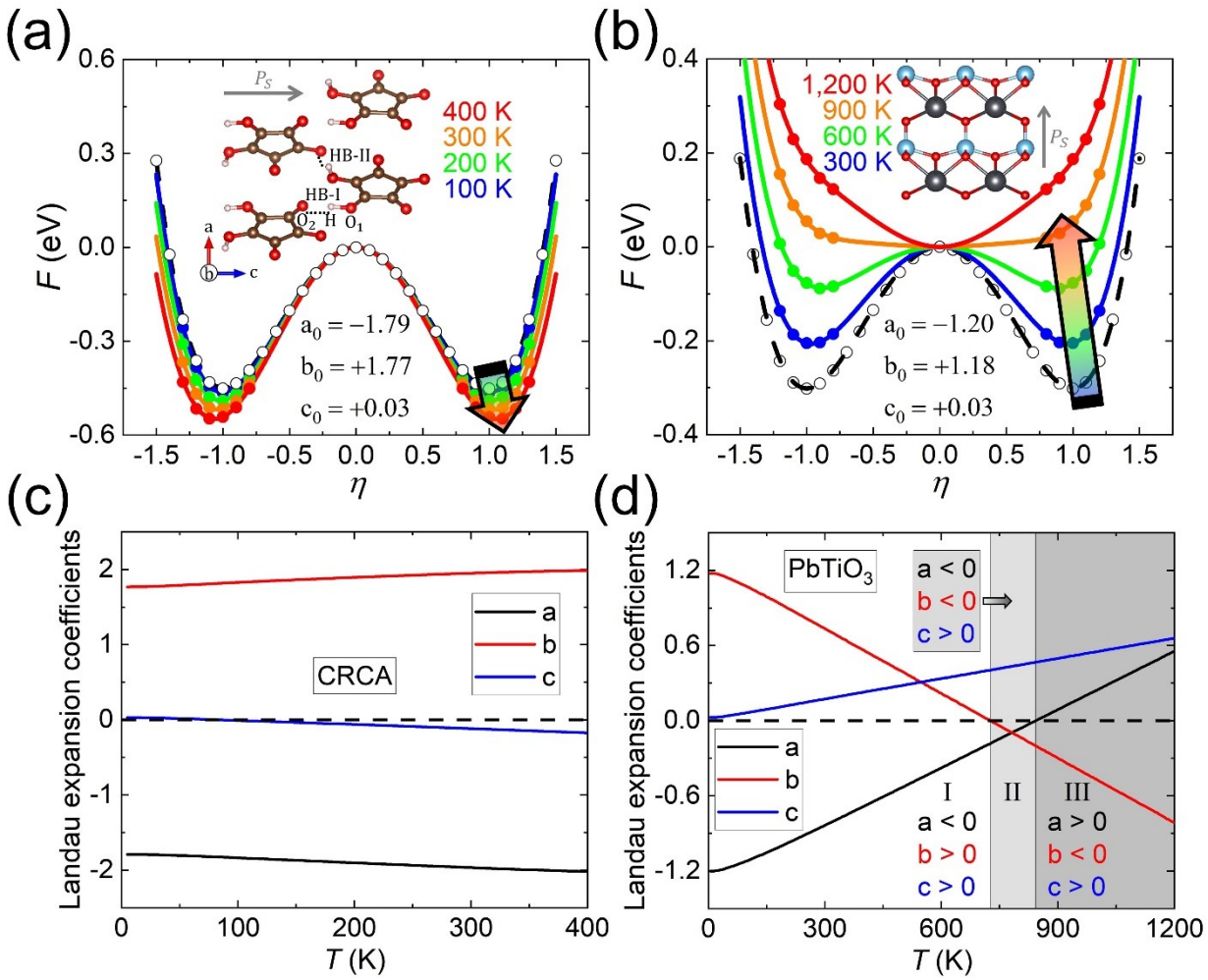


Fig. 1. (a, b) Free energy landscapes as a function of η at selected T for (a) CRCA, (b) $PbTiO_3$. Without loss of generality, η is taken as a linear interpolation between the ferroelectric ($\eta = 1$) and paraelectric ($\eta = 0$) structures. Solid circles represent free energies calculated at the quasi-harmonic level for structures near the ground-state ferroelectric phase that are free of imaginary phonon modes, and solid lines represent Landau free energy expansions fitted to the sixth order. The double-well potentials are shown by dashed lines. The insets show the unit-cell structures. P_S is along the polar direction $\hat{c}$. (c, d) T-dependent coefficients in the Landau free energy expansion $F(\eta, T) = F_0(T) + \frac{1}{2}a(T)\eta^2 + \frac{1}{4}b(T)\eta^4 + \frac{1}{6}c(T)\eta^6$. Here $F_0(T)$ is set to zero at each temperature. Note the negative correlation in sign between $\partial a/\partial T$ and $\partial \eta/\partial T$. Note that the expansion coefficients exhibit a nonlinear dependence on T at low temperatures, manifesting the nuclear quantum effect that is not included in AIMD simulations.

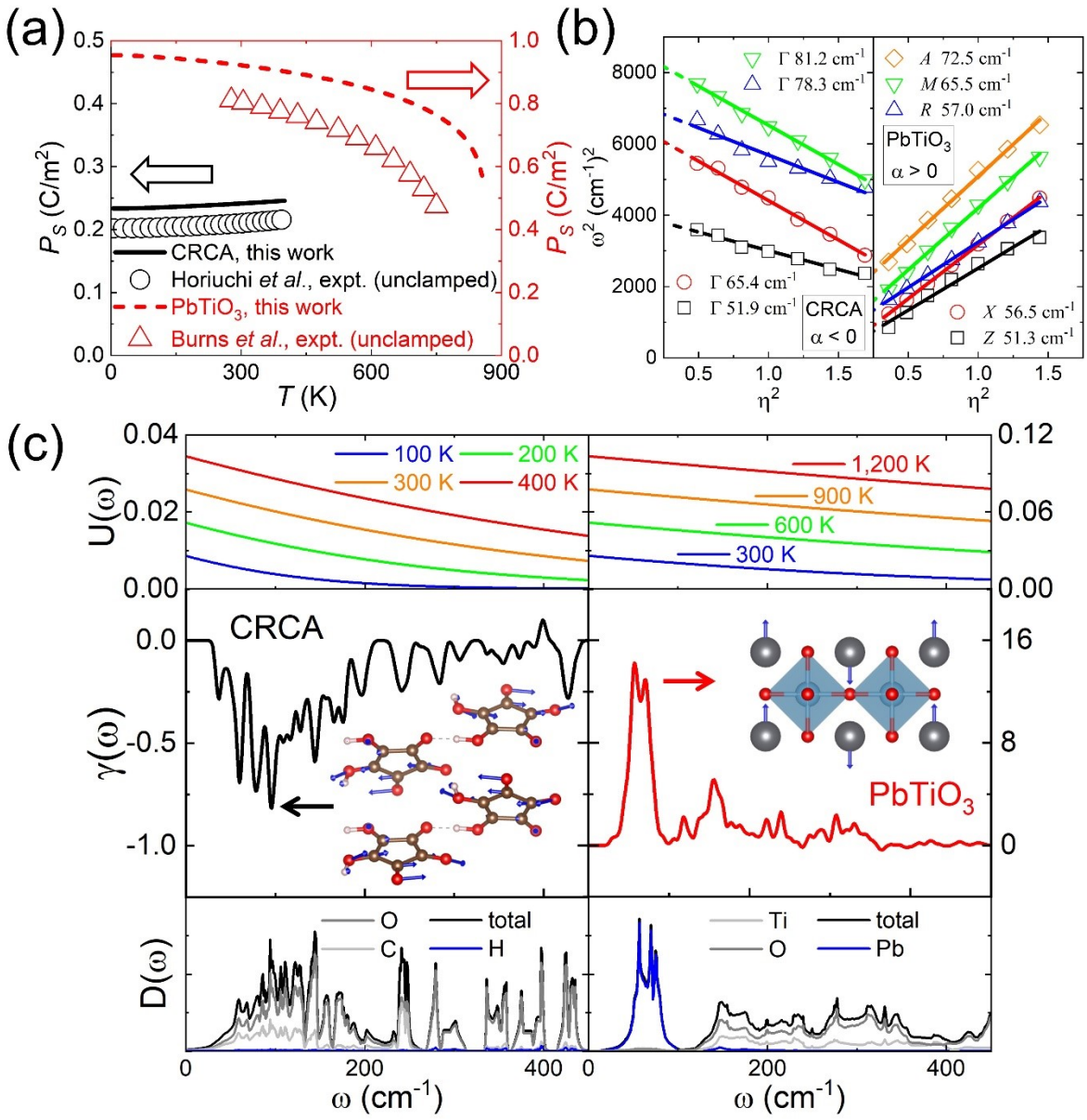


Fig. 2. (a) Clamped-lattice P_S as a function of T, for CRCA (left) and $PbTiO_3$ (right). A linear relation is used to convert η_T to P_S. (b) Dependence of the selected $\omega_{\vec{q}\lambda}(\eta)$ on η for CRCA (left panel) and $PbTiO_3$ (right panel). The relation follows $\omega^2_{\vec{q}\lambda}(\eta) = \omega^2_{\vec{q}\lambda}(\eta)|_{\eta=0} + \alpha_{\vec{q}\lambda}\eta^2$, with the negative (positive) sign of $\alpha_{\vec{q}\lambda}$ indicating the phonon stiffening (softening) upon transitioning from the ferroelectric structure to the paraelectric structure for CRCA ($PbTiO_3$). (c) From top to bottom: frequency-distributed internal energy $U(\omega)$, generalized Grüneisen parameter $\gamma(\omega)$, and phonon density of states $D(\omega)$ for CRCA (left panel) and $PbTiO_3$ (right panel). The inset shows the atomic displacement of representative low-frequency phonon mode with negative (positive) γ for CRCA ($PbTiO_3$). Neglecting the zero-point energy, $\partial F_{\text{vib}}(\eta, T)/\partial\eta = \sum_{\vec{q}\lambda} U_{\vec{q}\lambda}(\eta, T)\gamma_{\vec{q}\lambda}(\eta)$, where $U_{\vec{q}\lambda}$ is the vibrational internal energy $\hbar\omega_{\vec{q}\lambda}(\eta)n_{\vec{q}\lambda}$ and $n_{\vec{q}\lambda}$ is the Bose-Einstein distribution function. The right-hand side further yields $\int d\omega U(\omega)\gamma(\omega)D(\omega)$, where $U(\omega) = \hbar\omega n(\omega)$, and $\gamma(\omega)D(\omega) = \sum_{\vec{q}\lambda}\gamma_{\vec{q}\lambda}\delta(\omega - \omega_{\vec{q}\lambda})$.

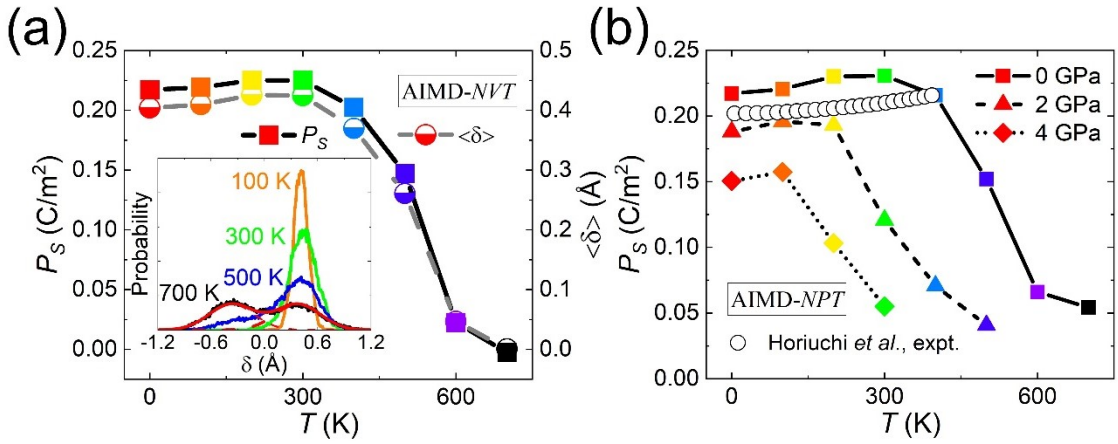


Fig. 3. (a) Pyroelectric responses calculated with AIMD simulations in the *NVT* ensemble. Main panel: ensemble-averaged P_S (left) and the defined order parameter δ (right) as a function of T. Inset: probability distribution of δ at selected T. At 700 K, the distribution (black) is well reproduced by the superposition of a bimodal off-centered gaussians (red), and the nature of the phase transition is hence identified to be of mostly order-disorder type. (b) P_S as a function of T at different pressures p, calculated with AIMD simulations in the *NPT* ensemble. At 0 GPa, a total Π of 50 μC/(m^2·K) is extrapolated below 300 K, in satisfactory agreement with the measured value of 55 ± 20 μC/(m^2·K), and the extrapolated T_C is around 550 K. Note that this phase transition is otherwise absent in experiments since CRCA crystal starts to decompose at elevated temperatures [16], the underlying mechanism of which is beyond the scope of this study since bond breaking is a rare event that is statistically not achievable by the present AIMD simulations. Note also that P_S falls to near but not zero due to the finite time and length scales achievable by the present AIMD simulations.